Superiority of localized surface plasmon resonance technique in characterization of ultra-thin metallic films

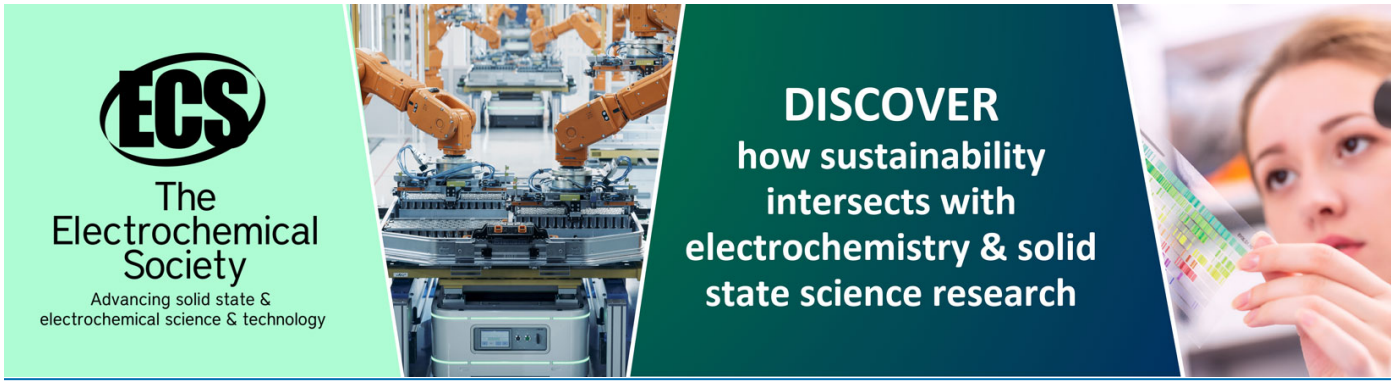

IOP Conf. Series: Journal of Physics: Conf. Series **961** (2018) 012013 doi:10.1088/1742-6596/961/1/012013

Superiority of localized surface plasmon resonance technique in characterization of ultra-thin metallic films

Sudheer[1,2,a], P. Tiwari[1,2], S. Bhartiya[2], C. Mukherjee[1,2], S. K. Rai[1,2], V. N. Rai[1,2,*], and A. K. Srivastava[1,2]

[1]Homi Bhabha National Institute, Mumbai, Maharashtra 400094, India
[2]Raja Ramanna Centre for Advanced Technology, Indore, Madhya Pradesh 452013, India

[a]E-mail: sudheer.rrcat@gmail.com, sudheer@rrcat.gov.in,
[*]Superannuated.

Abstract.The comparison and correlation of morphological, optical and crystallographic properties of ultra-thin Au films obtained using field-emission scanning electron microscopy (FESEM), x-ray reflectivity (XRR), UV-visible transmission, and grazing incidence x-ray diffraction (GIXRD) are presented. The Au thin films of different thickness are grown on the glass substrate using the sputtering technique. The particle size, number density and the covered area fraction of Au thin film are obtained from FESEM images. The XRR technique is used to determine the film thickness and surface roughness. The localized surface plasmon resonance (LSPR) response of Au thin films is obtained using UV-Vis transmission spectroscopy. The LSPR peak position and its strength are correlated with film morphology and thickness. Finally, it is shown that LSPR based spectroscopy techniques can provide much better information about morphology and thickness of the Au films up to a resolution of ~1 nm.

1. Introduction

The ultra-thin nanostructured metallic films of <10 nm thickness are of great interest because of their potential applications in nano-optics, energy harvesters like thin film solar cells and surface-enhanced Raman spectroscopy (SERS) [1,2,3,4]. The controlled fabrication of such nanostructured thin films along with accurate and fast characterization is very much crucial for its useful applications. Presently, among the various available techniques, fabrication of metallic thin film by the sputtering method has become popular due to its excellent control on the growth process [5]. The field-emission scanning electron microscopy (FESEM), and x-ray reflectivity (XRR) techniques are frequently used as the characterization tools for thin films. Amongst them, in FESEM, the charging effect and high vacuum requirement limit its applicability to conducting samples. The XRR technique provides accurate information about the thickness, surface and interface roughness, average mass density and electron density profile (EDP) of the continuous films [6,7]. But this technique did not provide significant information about the island and percolated type of films due to the absence of Keissing oscillations in the spectra. The localized surface plasmon resonance (LSPR) based spectroscopic technique that is the coherent oscillation of conduction band electron in nanostructures, is emerging as one of the superior tools especially for characterization of ultra-thin metal films (island and percolated) [8]. In the LSPR technique, optical transmission is dependent on particle size, shape, number density and the covered area fraction which can be further quantified for the characterization of ultra-thin films [9,10,11].

This article presents the comparison and correlation among various thin film characterization techniques. The LSPR based optical transmission is correlated with morphology and thickness of the film and found superior for characterization of the sputtered grown island and percolated films up to sub-nanometer resolution.

2. Experimental

The Au thin films are grown by a sputtering technique. The sputtering time was 10, 15, 20, 30, 45, and 60s at 10 mA current. The deposition was carried out on the glass substrate. Before the deposition process, a thorough cleaning of glass substrates was performed in a soap solution, acetone, and DI water. The characterizations of deposited films were carried out using FESEM, XRR, and UV-Vis transmission spectroscopy, and grazing-incident x-ray diffraction techniques (GIXRD). The ImageJ software is used to analyze the FESEM images. The Parratt formulation is applied for fitting the experimentally obtained XRR spectra [6].

3. Results and Discussion

3.1. *Morphological Characterization*

3.1.1. Imaging using scanning electron microscope

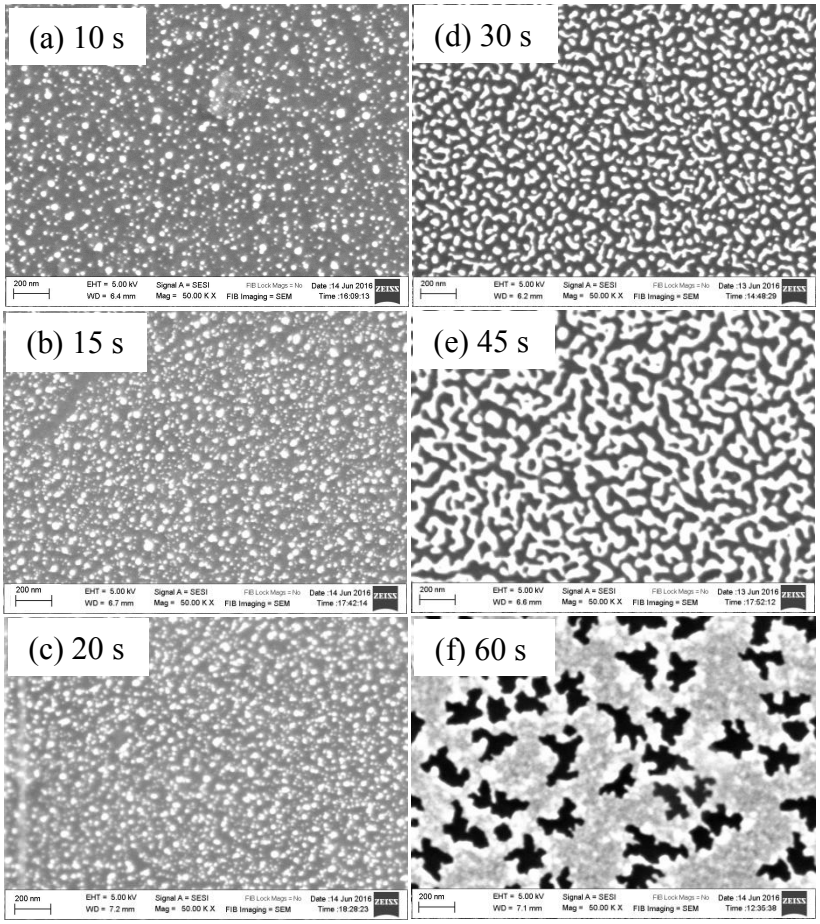

Figure. 1 Field-emission electron microscope image of Au thin films

First of all, the morphology of the fabricated Au thin films is imaged by FESEM. Figs. 1(a)-1(f) show the two-dimensional FESEM images of Au thin films of 10, 15, 20, 30, 45, and 60s samples. The quantitative analysis of FESEM images is performed in terms of average particle size (d) (Feret

Table-1: *Variation in particle size, number density, covered area fraction and thickness of Au thin film.*

Deposition time (s)	Particle size (nm)	Number density (particles /μm^{-2})	Covered area fraction (F%)	Thickness (nm)
10	24	3.74×10^2	13.66	1.4
15	25	6.55×10^2	19.31	2.1
20	29	5.29×10^2	23.99	2.8
30	72	1.62×10^2	33.63	4.2
45			52.45	6.3
60			72.75	8.4

diameter), number density (n), and covered area fraction (F%) [Table-1]. The Feret diameter is defined as d=P/π, where P is the perimeter of Au nanoparticle [12]. Figs. 1(a)-1(b) show the average particle size is almost same, and shape is nearly spherical for 10 and 15s films while the particle number density in the 15s film is almost twice in comparison to the 10s film (Table-1). For the 20s film, particle size increases while number density decreases. It is widely reported in the literature that both of the above facts probably occurs only due to coalescence phenomenon. In which the nearest neighbor small particles come in the contact and form bigger particles. In the case of 30s film average particle sizes abruptly increases. In which the small sizes particle have a nearly spherical shape while larger size particles have complex chain-like structures. The few bigger chains structure has sizes ~280 nm also exist. In case of the 45s sample, size of the complex chain structures are further increases, and interconnected networks are formed in the film. Such kind of films are well known as percolated films. After that in the case of 60s sample, the percolated structures finally transformed in the continuous patches of films (semicontinuous film). The covered area fraction (F%) for 10s sample is found ~14 %. It to be noted that F% consistently increases with the deposition time and reaches up to ~73 % for 60s sample.

3.1.2. X-ray reflectivity

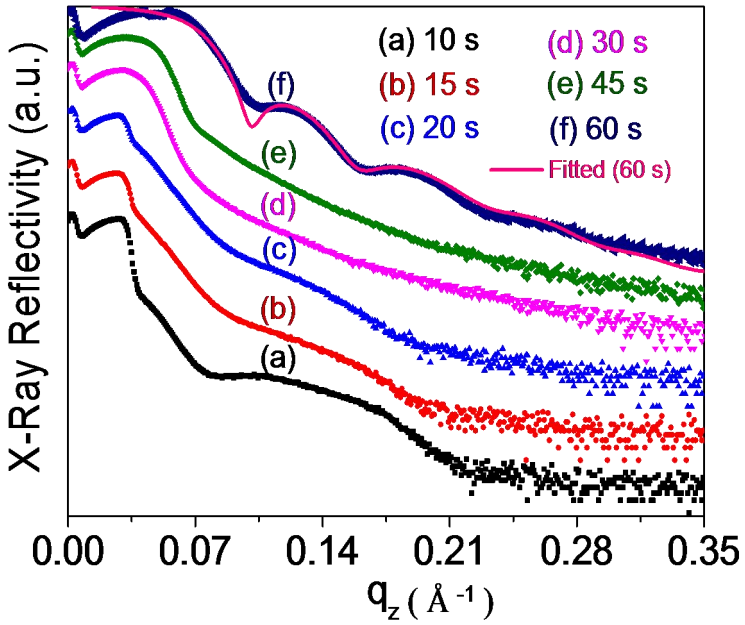

Fig. 2 X-ray reflectivity spectra of sputter grown Au thin films

Fig. 2 shows the XRR spectra of Au thin film deposited for different times. For 60s sample, well defined Keissing oscillations are found in the XRR spectra [7]. The experimental data of 60s sample is fitted with simulated data. The thickness and roughness values are estimated as 8.4 nm and 1.3 nm respectively. As described above that 60s sample shows the presence of large patches of continuous film in the FESEM images (Fig. 1(f)). These patches are supportive in XRR measurement and produce oscillation in the recorded spectra. These oscillations damped for all other films (10-45s) due to an island or percolated structures (Figs. 1(a)-1(e)). The island and percolated structure reduces the specular reflection and enhances the scattering of the incident x-ray beam that results in vanished Keissing oscillations in the spectra. Therefore, XRR technique is limited for semicontinuous and continuous films. Only a small information can be extracted for island or percolated films from the XRR technique. Thus, for all other lower thickness films, average mass-thickness is determined by scaling with time and shown in Table-1[12,13].

3.2. Optical characterization

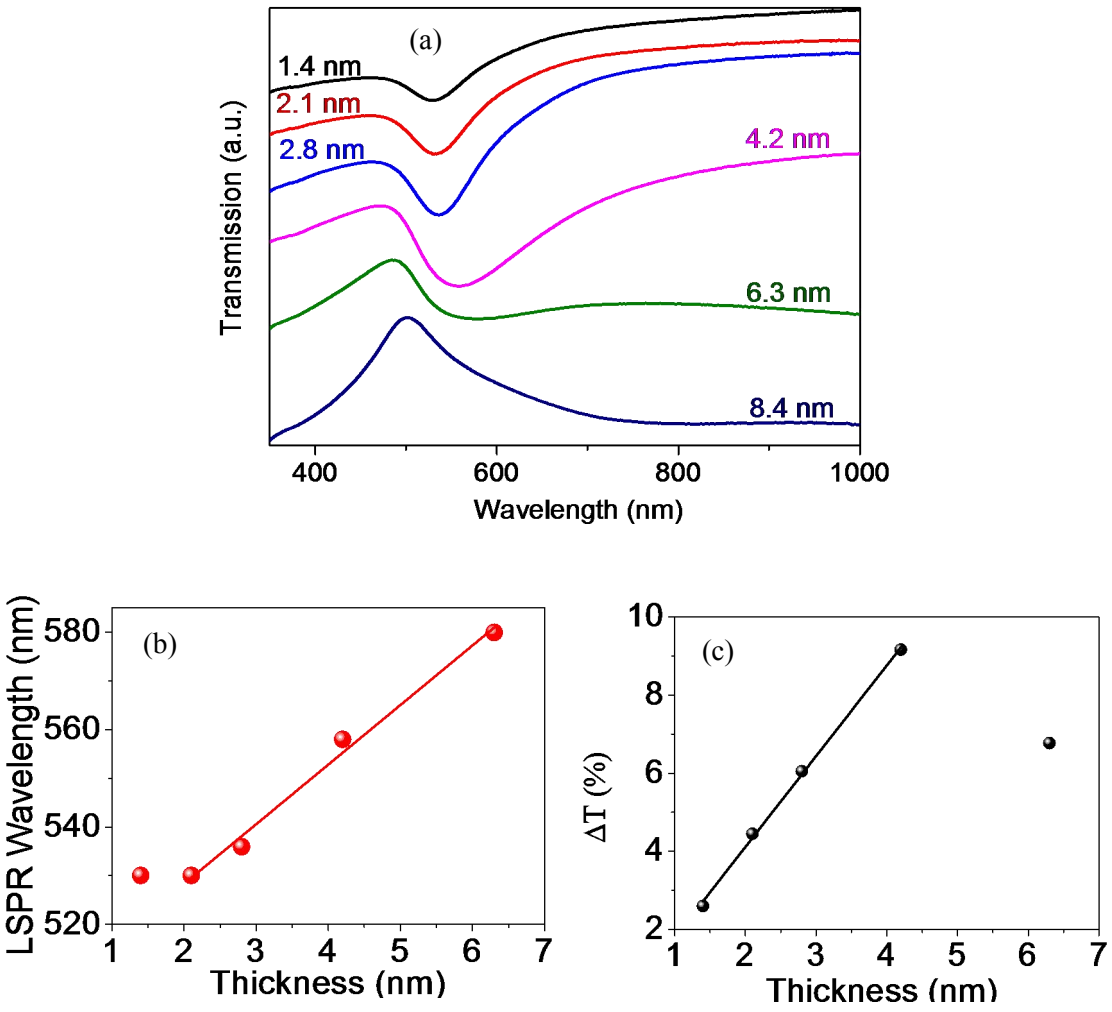

Fig. 3 (a) UV-Vis transmission spectra of Au thin films, (b) variation in LSPR dip position with film thickness and (c) variation in LSPR dip strength with film thickness.

To verify the above scaling rule of thickness and to explore the superiority of LSPR based technique, the transmission spectra of the Au thin films are recorded. Fig. 3(a) shows the transmission spectra of sputtered grown Au thin films. A dip at ~530 nm wavelength in the transmission spectra is found for

1.4 nm thickness film. This fall in the transmission spectra is due to the presence of random Au islands in the films showing excitation of characteristic LSPR. The LSPR minima position and its broadening are intimately dependent on size and shape of the nanoparticles as well as their decoration on the substrate. A similar LSPR peak position in the 1.4 nm and 2.1 nm thickness film is the clear evidence of the existence of the same particle size. A variation in particle number density is strongly witnessed to increase the LSPR strength in 2.1 nm thickness films. Moreover, a small change in the participle size distribution can produce inhomogeneous broadening in the LSPR profile which can be realized by variation in its full width at half maxima (FWHM). The increment in the particle size leads to a consistent redshift of LSPR peak position of the film as thickness increases from 2.1 to 4.2 nm (Fig. 3(a)). The 6.3 nm thickness film shows the convoluted optical response of both island and percolated film. Finally, in the case of 8.4 nm thickness film, spectra become like a typical optical response of highly percolated films. Furthermore, the optical response of Au thin films is quantified in terms of peak position (λ), and its strength (ΔT%) according to the methodology described in the literature [10,11,13]. Figs. 3(b)-3(c) show the variation in λ and ΔT% with thickness. All the experimentally obtained data are fitted linearly with slopes 12.3 ±0.8 and 2.3± 0.1 % respectively. It is well known that most of the spectrophotometer has wavelength and transmittance resolution of ~1 nm and 0.1 % respectively. Which clearly indicated that thickness of the ultra-thin metal films can be obtained with the resolution of sub-nanometer scale.

3.3. Crystallographic characterization

The GIXRD spectra were also recorded for 1.4, 2.8, 4.2 and 8.4 nm thickness Au thin films. The peaks in the XRD spectra are indexed as (111), (200), (220) and (311) planes of face-centered cubic (FCC) Au crystal structures[14]. The spectra indicate that for <4.2 nm thickness film GIXRD technique could also not deliver the significant information about the crystal structure and grain size present in the film.

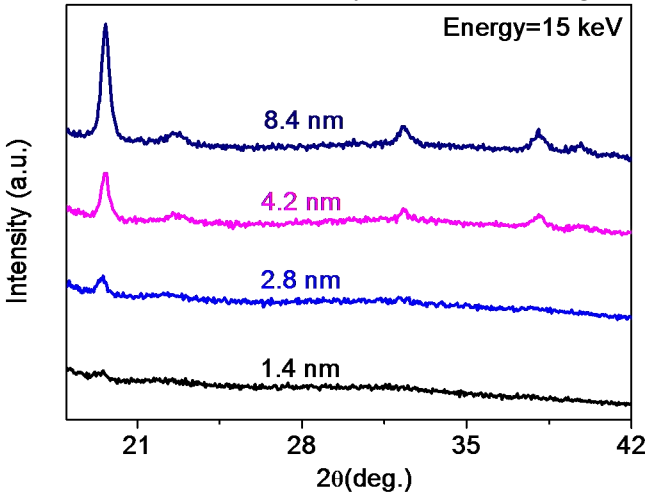

Fig. 4 X-ray diffraction spectra of Au thin films

4. Conclusions

The sputter grown Au thin films of thickness <10 nm have been characterized using various techniques. The morphology and thickness of the film are obtained by FESEM and XRR techniques. The localized surface plasmon resonance (LSPR) response is measured using UV-Vis optical transmission, and their results are quantified and correlated with the morphology and thickness. The correlation suggests that LSPR technique can be used to find the film thickness up to sub-nanometer resolution. Finally, LSPR based characterization is found to be a superior technique for characterization of ultra-thin Au films.

Acknowledgment:
One of the authors Sudheer acknowledges the Homi Bhabha National Institute (HBNI) for providing financial assistance. Authors are thankful to Mr. Mahendra Babu for providing help during the deposition of Au thin films. Authors are also thanked Mr. Rajiv Kamparath for providing active guidance during optical measurements.

References

[1] K. Wen, Y. Hu, L. Chen, J. Zhou, L. Lei and Z. Guo, Opt. Comm. **336**, 243 (2015).
[2] Y. A. Akimov, W. S. Koh, K. Ostrikov, Opt. Exp. **17**, 10195 (2009).
[3] A. Merlen, V. Gadenne, J. Romann, V. Chevallier, L. Patrone, J. C. Valmalette, Nanotechnology **20**, 215705 (2009).
[4] G. Q. Liu, Z. Q. Liu, Y. H. Chen, K. Huang, L. Li, F. L. Tang, L. X. Gong, Y. Hu, X. N. Zhang, Optik **124**, 5124 (2013).
[5] T. D. Phuc, M. Yoshine, A. Yamanaka, and T. Yamamoto, Int. J. of Automation Technology **8**, 1 (2013).
[6] L. G. Parratt and C. F. Hempstead, Phy Rev. Lett. **94**, 1593 (1594).
[7] I. Stabrawa, D. Banas, K. Dworecki, A. Kubala-Kukus, J. Braziewicz, U. Majewska, J. Wudarczyk-Mocko, M. Pajek and S. Gózdz, ACTA PHYSICA POLONICA A **129**, 233 (2016).
[8] A. Herz, A. Franz, K. Theska, M. Hentschel, Th. Kups, D. Wang, and P. Schaaf, AIP Advances **6**, 035109 (2016).
[9] U. Kreibig and M. Vollmer, Optical Properties of Metal Clusters (Springer, Heidelberg, 1995).
[10] Gong, Y. Zhou, L. He, B. Xie, F. Song, M. Han and G. Wang, Eur. Phys. J. D **67**: 87 (2013).
[11] S. Verm, B. T. Rao, S. Bhartiya, V. Sathe, L. M. Kukreja, App. Surf. Sci. **346**, 379 (2015).
[12] Sudheer, Puspen Mondal, V. N. Rai, and A. K. Srivastava, AIP Advances **7**, 075303 (2017).
[13] S. Verma, B. T. Rao, S. Rai, V. Ganesan, and L. M. Kukreja, Appl. Sur. Sci. **258**, 4898 (2012).
[14] V. Svorcík, O. Kvítek, J. Ríha, Z. Kolská, J. Siegel, Vacuum **86**, 729 (2012).